Published in final edited form as:
Drug Dev Res. 2013 March ; 74(2): 65–80. doi:10.1002/ddr.21063.

Anti-Oligomannose Antibodies as Potential Serum Biomarkers of Aggressive Prostate Cancer

Denong Wang[1,2,*], **Laila Dafik**[1,2], **Rosalie Nolley**[3], **Wei Huang**[4], **Russell D. Wolfinger**[5], **Lai-Xi Wang**[4], and **Donna M. Peehl**[3]

[1]Tumor Glycomics Laboratory, SRI International Biosciences Division, 333 Ravenswood Avenue, Menlo Park, CA 94025, USA

[2]Stanford University School of Medicine, Stanford, CA 94305, USA

[3]Department of Urology, Stanford University School of Medicine, Stanford, CA 94305, USA

[4]Institute of Human Virology and Department of Biochemistry & Molecular Biology, University of Maryland School of Medicine, Baltimore, MD 21201, USA

[5]SAS Institute Inc., SAS Campus Drive, Cary, NC 27513, USA

Abstract

Strategy, Management and Health Policy				
Enabling Technology, Genomics, Proteomics	Preclinical Research	Preclinical Development Toxicology, Formulation Drug Delivery, Pharmacokinetics	Clinical Development Phases I-III Regulatory, Quality, Manufacturing	Postmarketing Phase IV

This study bridges a carbohydrate microarray discovery and a large-scale serological validation of anti-oligomannose antibodies as novel serum biomarkers of aggressive prostate cancer (PCa). Experimentally, a Man9-cluster-specific enzyme-linked immunosorbent assay was established to enable sensitive detection of anti-Man9 antibodies in human sera. A large-cohort of men with PCa or benign prostatic hyperplasia (BPH) whose sera were banked at Stanford University was characterized using this assay. Subjects included patients with 100% Gleason grade 3 cancer (n = 84), with Gleason grades 4 and/or 5 cancer (n = 204), and BPH controls (n = 135). Radical prostatectomy Gleason grades and biochemical (PSA) recurrence served as key parameters for serum biomarker evaluation. It was found that IgG^{Man9} and IgM^{Man9} were widely present in the sera of men with BPH, as well as those with cancer. However, these antibody reactivities were significantly increased in the subjects with the largest volumes of high grade cancer. Detection of serum IgG^{Man9} and IgM^{Man9} significantly predicted the clinical outcome of PCa post-radical prostatectomy. Given these results, we suggest that IgG^{Man9} and IgM^{Man9} are novel serum

*Correspondence to: Denong Wang, Tumor Glycomics Laboratory, Center for Cancer Research, SRI International Biosciences Division, 333 Ravenswood Avenue, Menlo Park, CA 94025, USA. denong.wang@sri.com.

biomarkers for monitoring aggressive progression of PCa. The potential of oligomannosyl antigens as targets for PCa subtyping and targeted immunotherapy is yet to be explored.

Keywords

autoantibodies; carbohydrate microarray; oligomannose; prostate cancer

INTRODUCTION

Prostate cancer (PCa) is the most common non-cutaneous malignancy in men. Based on autopsy studies, a significant number of American men in their 30s already have cancer in their prostates; this frequency rises to about 80% for men in their 70s. Despite such a high incidence of PCa, only 8% of men in the United States in their lifetime present with clinically significant disease that affects their quality of life [Stamey et al., 1993], and only 3% of all men in the United States die of PCa [Ries, 1994]. No other human cancer possesses such an enormous disparity between the very high incidence of malignancy microscopically and the relatively low death rate. For example, breast cancer, the leading female malignancy, commands a 15% mortality rate within 5 years [DeSantis et al., 2011a, 2011b], while lung cancer, the third most common malignancy overall, commands an overwhelming 86% mortality rate within 5 years [Bach et al., 2004].

Such a striking disparity between the high incidence of occurrence and relatively low rate of death from PCa has prompted us to ask: (i) are there mechanisms of host surveillance that substantially reduce the death rate from PCa; (ii) can novel assays be established to detect the high-risk, high-mortality status of PCa so that effective treatment can be given to these subjects to reduce the death rate from the disease; and (iii) are there key immunological targets that are differentially expressed among aggressive cancer (aPCa) and other clinically indolent, nonaggressive cancers (iPCa)? Identification of such immunogenic elements is crucial for establishment of therapeutic and diagnostic strategies to improve current health care of PCa patients.

Our group has been investigating the potentially immunogenic carbohydrate moieties of PCa. Assessing patterns of lectin binding to tissue microarrays, we observed abnormal expression of a number of glycan markers in PCa [Wang et al., 2011]. These markers were the precursors, cores, and internal sequences of *N*-glycans, such as oligomannoses, triantennary type II (Galβ1→4GlcNAc) chains (Tri-II), or multivalent type II chains (m-II) [Wang, 2012]. A common immunological characteristic of these markers is that they are usually masked by other sugar moieties, and they belong to a class of glyco-epitopes that are normally “cryptic.” Importantly, their tissue expression or amounts of exposure appear to differ dramatically among different Gleason grades of PCa and tumor metastases [Wang et al., 2011; Lange et al., 2012]. This is of potential clinical significance because Gleason grade is the strongest predictor of recurrence of PCa following definitive surgical or radiation therapy.

Subsequently, we found in an animal model study that a tumor cell-based vaccine elicited anti-Man9-cluster antibodies [Newsom-Davis et al., 2009]. In this case, Fas-ligand-

transfected melanoma cells were used for animal immunization. A monoclonal antibody (mAb) TM10 established by this immunization strategy illustrates a unique binding profile in flow cytometry analysis. TM10 does not bind to the cell surface of untransformed normal cells but strongly binds a number of murine and human tumor cell lines, including those from melanoma, prostate, breast and ovarian cancers. Interestingly, our carbohydrate microarray analysis revealed that TM10 recognizes the oligomannosyl epitopes presented by (Man9)n-*Keyhole limpet hemocyanin* (KLH) and [(Man9)4]n-KLH [Newsom-Davis et al., 2009]. These glyco-conjugates were initially constructed to display an HIV-1 neutralization epitope recognized by mAb 2G12 [Ni et al., 2006] but were found in this study to present the tumor-associated TM10-antigens.

Using carbohydrate microarrays, we further examined whether human immune systems also recognize these tumor carbohydrates and mount antibody responses. We analyzed a panel of sera from men with PCa ($n = 17$) compared with sera from men with benign prostatic hyperplasia (BPH) ($n = 12$). The two TM10-positive Man9-conjugates were found to be highly effective in capturing human serum IgG antibodies from both of these groups. However, the levels of antibodies captured in the cancer group were significantly higher than those detected in the BPH group [Wang, 2012].

Taken together, these findings suggested that the tumor-associated TM10 antigens are potentially immunogenic in vivo. Abnormal expression or exposure of these targets may trigger specific autoantibody responses in cancer subjects. To further evaluate this hypothesis, we extended our investigation to a larger-scale serological study using the Stanford cohort of radical prostatectomy specimens and sera. As summarized below, we have established an enzyme-linked immunosorbent assay (ELISA) to enable highly specific detection of anti-Man9-cluster antibodies, including IgG^{Man9} and IgM^{Man9}, in human sera. We have confirmed that anti-Man9-cluster antibodies are widely present in human circulation, and that the levels of these autoantibodies significantly increase in men whose cancers contain a large volume of Gleason grades 4 and/or 5.

MATERIALS AND METHODS

The Stanford Cohort of Radical Prostatectomy Specimens and Sera

This cohort included men whose cancers were known to be composed entirely of Gleason grade 3 (Gr3) ($n = 84$), men whose cancers contained 1.0–100% Gleason grades 4 and/or 5 (Gr4/5) cancer ($n = 204$), and the BPH controls who were biopsy-confirmed to be negative for PCa ($n = 135$). The BPH cohort was selected from men who had undergone two rounds of systematic prostate biopsies to rule out the presence of cancer. The cancer cohort was selected from men who had undergone radical prostatectomy at Stanford and whose prostates were sectioned at 3-mm step intervals and quantitatively characterized for eight morphological variables [Stamey et al., 1993, 1999]. Mean age was 67.3 (47–88), 61.35 (37–75), and 63.73 (41–80) years for BPH, Gr3, and Gr4/5, respectively. Mean of follow-up days was 2437.63 (221–4884) for Gr3 and 2374.27 (292–6174) for Gr4/5, with failure defined as biochemical (PSA) recurrence. All patients were consented with Institutional Review Board-approved protocols.

Specimens used were banked at Stanford University between 1984 and 2006. Blood was obtained during the preoperative consultation prior to radical prostatectomy and collected in tubes with silica clot activator. Following centrifugation, the sera were collected and stored at −80°C as aliquots until analysis. Sera from men with BPH were obtained during office visits to the Stanford Department of Urology for symptoms of BPH. All were biopsied at least twice and confirmed to be negative for cancer.

Carbohydrate Antibodies and Antigens

MAb TM10 [Newsom-Davis et al., 2009] was kindly provided by Dr. Thomas E. Newsom-Davis and mAb 2G12 by the NIH AIDS Research and Reference Reagent Program. A biotinylated anti-human IgM antibody, an alkaline phosphatase (AP)-conjugated anti-human IgG, and a horseradish peroxidase (HRP)-streptavidin conjugate were purchased from Sigma-Aldrich (St. Louis, MO, USA). Biotinylated Concanavalin A (Con A) was purchased from EY Laboratories, Inc. (San Mateo, CA, USA). The carbohydrate antigens and glycoconjugates that were previous described are summarized in Table 1.

Synthesis and Characterization of Oligomannosyl Conjugates

$Man_9GlcNAc_2Asn$ and $Man_5GlcNAc_2Asn$ were prepared following the reported method [Wang et al., 2004]. (Man9)n-KLH and [(Man9)4]n-KLH were prepared as previously described [Ni et al., 2006]. The synthesis of the glycoconjugates, (Man5)n-BSA and (Man9)n-BSA, is described in the following procedures:

High-performance liquid chromatography (HPLC)—Analytical RP-HPLC was performed on a Waters 626 HPLC instrument with a Symmetry300™ C_{18} column (5.0 μm, 4.6 × 250 mm; Waters Corporation, Milford, MA) at 40°C. The Symmetry300 column was eluted with water containing 0.1% TFA within 10 min at a flow rate of 1 mL/min (*Method A*). Preparative HPLC was performed on a Waters 600 HPLC instrument with a preparative Symmetry300™ C_{18} column (7.0 μm, 19 × 250 mm). These columns were eluted with water containing 0.1% TFA at a flow rate of 12 mL/min.

Mass spectrometry (MS)—The ESI-MS Spectra were measured on a Waters Micromass ZQ-4000 single quadruple mass spectrometer.

$Man_9GlcNAc_2Asn$-maleimide—A solution of $Man_9GlcNAc_2Asn$ (20 mg) and N-(beta-Maleimidopropyloxy)succinimide ester (BMPS) (26 mg) in a phosphate buffer (50 mM, 3 mL, pH 7.4) containing 20% acetonitrile was stirred at 23°C for 3 hours. The residue was subject to the preparative HPLC purification to give the product $Man_9GlcNAc_2Asn$-maleimide (20 mg, 93%). Analytical HPLC (*Method A*): t_R = 5.7 min; ESI-MS: calculated M = 2149; found 1076.1 $[M + 2H]^{2+}$.

$Man_5GlcNAc_2Asn$-maleimide—A solution of $Man_5GlcNAc_2Asn$ (3 mg) and BMPS (6 mg) in a phosphate buffer (50 mM, 0.35 mL, pH 7.4) containing 20% acetonitrile was stirred at 23°C for 3 hours. The residue was subjected to the preparative HPLC purification to give the product $Man_5GlcNAc_2Asn$-maleimide (2.6 mg, 78%). Analytical HPLC (method A): t_R = 5.5 min; ESI-MS: calculated M = 1501; found 751.2 $[M + 2H]^{2+}$.

BSA-SH—A mixture of BSA (40 mg) and 2-iminothiolane (20 mg) in a phosphate buffer (50 mM, 2 mL, pH 7.2, containing 5 mM EDTA) was shaken at 23°C for 2 hours. The residue was subject to size-exclusion chromatography on a Sephadex G-25 (Sigma, St. Louis, MO) column. The column was eluted with a phosphate buffer (20 mM, pH 7.2). The protein fractions were combined and quantified by Bradford protein assay (for protein quantity) and free sulfhydryl assay using Ell-man's reagent (for free thiol quantity). The resultant BSA-SH was 41 mg containing 32.6 μM free thiol groups.

(Man9)n-BSA—A solution of BSA-SH (41 mg, containing 32.6 μM free thiols) and $Man_9GlcNAc_2$Asn-maleimide (10 mg) in a phosphate buffer (20 mM, 10 mL, pH 7.2, containing 5 mM EDTA) was shaken at 23°C for 3 hours. The solution was lyophilized and the residue was subjected to size-exclusion chromatography on a Sephadex G-25 column. The column was eluted with phosphate buffer (10 mM, pH 6.6). The protein fractions were combined to give the $Man_9GlcNAc_2$-BSA (40 mg). The carbohydrate component was quantified by anthrone assay (6.1 mg carbohydrates, 15% w/w in total $Man_9GlcNAc_2$-BSA).

(Man5)n-BSA—A solution of BSA-SH (6 mg, containing 4.8 μM free thiols) and $Man_5GlcNAc_2$Asn-maleimide (2.5 mg) in phosphate buffer (20 mM, 1.5 mL, pH 7.2, containing 5 mM EDTA) was shaken at 23°C for 3 hours. The residue was subjected to size-exclusion chromatography on a Sephadex G-15 column. The column was eluted with phosphate buffer (10 mM, pH 6.6). The protein fractions were combined to give the $Man_5GlcNAc_2$-BSA (6 mg). The carbohydrate component was quantified by anthrone assay (1.15 mg carbohydrates, 19% w/w in total $Man_5GlcNAc_2$-BSA).

Carbohydrate Microarrays

Carbohydrate antigens of various complexities were dissolved in phosphate-buffered saline (PBS) (glyco-protein conjugates) or saline (polysaccharides), and spotted onto SuperEpoxy 2 Protein slides (ArrayIt Corporation, Sunnyvale, CA, USA) by a high-precision robot designed to produce cDNA microarrays (Cartesian Technologies' PIXSYS 5500C, Irvine, CA). Immediately before use, the printed microarray slides were washed in 1XPBS at room temperature (RT) for 5 minutes, and blocked with 1%BSA-PBS at RT for 30 minutes. They were then incubated with 50 μL of antibodies or lectins (as described in Fig. 1 legend) at RT for 1 hour followed by washing and then incubated with titrated secondary antibodies or streptavidin conjugates with distinct fluorescent tags, Cy5, PE, or FITC, at RT for 30 minutes. The stained slides were rinsed five times and spin-dried at room temperature before scanning for fluorescent signals. The ScanArray5000A Microarray Scanner (PerkinElmer Life Science, Boston, MA) was used to scan the stained microarrays. Fluorescent intensity values for each array spot and its background were calculated using ScanArray Express software (PerkinElmer Life Science).

Antigen-Specific ELISA Assays

A protocol described previously [Wang et al., 2002] for detection of anticarbohydrate antibodies was followed with minor modifications. In brief, (Man9)n-BSA or (Man5)n-BSA was diluted in 0.1 M sodium bicarbonate buffer solution, pH 9.6, for coating on ELISA microplates followed by blocking using 1% BSA, PBST. Human serum was diluted at 1:500

in 1% BSA, PBST for ELISA. The bound anti-Man9-cluster antibodies were revealed by a combination of conjugated secondary antibodies, including an AP-conjugate of goat anti-human IgG-Fc-specific antibody and a biotinylated goat anti-human IgM-Fc-specific antibody followed by HRP-streptavidin-conjugate.

Statistical Analyses

SAS Institute's JMP and JMP-Genomics software (Cary, NC, USA) were applied in the following analyses:

Carbohydrate microarrays—Microarray datasets collected by ScanArray Express were further analyzed using JMP-Genomics. In Figure 1, the antibody/lectin binding reactivity is shown as microarray scores, which are the log2 transformed mean microarray values of triplicate detections. The binding profile for each binder was shown as an overlay plot of the microarray scores for the spotted antigens in the same carbohydrate microarray. A cutoff to detect significant differences from the mean of background is determined by applying a multiple testing correction to statistical results from the analysis of variance (ANOVA) model.

ELISA—One-way ANOVA was performed to compare the ELISA results obtained among groups and/or subgroups. A nonparametric statistical test (Wilcoxon rank-sum method) was applied to calculate the significance of differences among comparative groups (Fig. 3, Tables 3 and 4). Least Squares Fit analysis in Fit Model mode was applied to estimate the weight of a serum marker or a combination of markers in predicting the percentage or volume of Gr4/5 cancer. Nominal Logistic Fit model was applied to investigate the performance of a serum marker as a classifier for differential diagnosis of PCa or prognosis of clinical outcome of the disease (Figs 5 and 6). Restricted maximum likelihood method was applied in associations and multivariate analyses to estimate the performance of serum markers in combination (Fig. 7).

RESULTS

Design and Construction of a TM10-Tumor Antigen

The two neoglycoconjugates that we applied in previous microarray studies, (Man9)n-KLH and [(Man9)4]n-KLH, were constructed to study immune responses to HIV-1 carbohydrates [Ni et al., 2006; Newsom-Davis et al., 2009; Wang et al., 2011]. In an immunoassay, the KLH carrier would have the disadvantage of capturing irrelevant anti-KLH antibodies if such specificities were present in human sera. We therefore constructed an additional neoglycoconjugate, (Man9)n-BSA, to selectively detect anti-Man9-cluster antibodies.

To determine whether (Man9)n-BSA preserved the tumor-specific TM10-glyco-epitopes, we characterized this compound in a carbohydrate microarray analysis (Fig. 1 and Table 2). The structural characteristics of the three high-mannose-conjugates are shown in Figure 1A. (Man9)n-BSA (1.) is similar to (Man9)n-KLH (2.) in the linkage used for coupling oligoman-noses to a protein carrier and in the molar ratio between the Man9 unit and corresponding carrier. By contrast, [(Man9)4]n-KLH (3.) was constructed by introducing a

defined scaffold to display the tetra-valent oligomannose clusters in order to mimic the high-density Man9-clusters expressed by the gp120 glyco-protein of HIV-1 [Li and Wang, 2004; Ni et al., 2006]. Its expression of the HIV-1-specific glyco-epitopes is determined by binding to an HIV-1 neutralization mAb 2G12 [Trkola et al., 1996; Sanders et al., 2002; Scanlan et al., 2002; Wang and Herzenberg, 2011].

Figure 1B–D show microarray binding profiles of Con A, TM10, and 2G12, respectively. As expected, the three Man9-cluster conjugates are similarly reactive with Con A (Fig. 1B) but are differentially reactive with 2G12 (Fig. 1D). Con A detects terminal mannoses with the C-3, C-4, and C-5 hydroxyl groups [Goldstein et al., 1965]. Its binding to these conjugates is, thus, independent of the Man9-cluster configurations. [(Man9)4]n-KLH is highly and selectively bound by 2G12 (Fig. 1D), which reflects its expression of the HIV-1-specific M9(2G12) glyco-epitopes. Differing from [(Man9)4]n-KLH, (Man9)n-BSA and (Man9)n-KLH are highly reactive with anti-tumor mAb TM10 (Fig. 1C). Thus, this microarray analysis confirms that the newly designed glyco-conjugate, (Man9)n-BSA, preserves well the TM10-reacting epitopes. Given that (Man9)n-BSA and (Man9)n-KLH differ in the protein carrier, the TM10-glyco-epitopes are clearly presented by their common Man9-cluster components. As the two TM10-positive conjugates are only marginally reactive with 2G12, the tumor-associated TM10-epitopes differ from the HIV-1-specific 2G12-glycoepitopes.

Establishment of a Highly Specific ELISA for Detection of TM10-Like Antibodies

We further examined whether (Man9)n-BSA is suitable for an ELISA platform to support specific detection of TM10-like anti-Man9-cluster antibodies. For this investigation, we constructed an additional glyco-conjugate, (Man5)n-BSA. As shown in Figure 2A, (Man9)n-BSA and (Man5)n-BSA share the Man5GlcNAc2Asn-moiety and the linkage used to couple them to the BSA molecule. Differing from Man9, which displays Manα1,2Man-moieties in the nonreducing ends, Man5 expresses no terminal Manα1,2Man-moiety but presents Manα1,3Man and Manα1,6Man moieties at its terminals.

Figure 2B and C show ELISA-binding curves of Con A and TM10, respectively, on microtiter plates coated with (Man9)n-BSA and (Man5)n-BSA. The plates were coated with a series of dilutions of the glyco-conjugates and reacted with a constant concentration of TM10 or Con A. Such an assay design is practical for epitope-mapping and measurement of the relative binding affinity of carbohydrate–anticarbohydrate interactions. In this analysis, Con A was used to monitor whether the two glyco-conjugates were quantitatively immobilized on the ELISA plates and whether their oligomannosyl moieties were accessible for specific binding. Figure 2B shows that Con A-binding curves with (Man9)n-BSA and (Man5)n-BSA are near linear in the ranges of antigen concentrations from 0.25 to 10.00 μg/mL. Both conjugates appear to be stably immobilized on ELISA plates with their terminal mannoses readily reactive with Con A. Figure 2C shows that TM10 is highly and selectively reactive with (Man9)n-BSA but has no binding to (Man5)n-BSA. Its Man9-binding curve is near linear in the range of antigen concentrations from 1.0 to 20.00 μg/mL. Thus, although both conjugates display Con A-epitopes, only (Man9)n-BSA preserves the tumor-specific TM10-glyco-epitopes.

Subsequently, we investigated the ELISA conditions for measuring anti-Man9-antibodies in human serum. In Figure 3, we show ELISA results with 436 sera measured at a constant dilution of 1:500 in 1% BSA PBST. This condition was determined in preliminary experiments to maximize the ratio of anti-Man9 signal (Ig^{Man9}) to the assay background (Ig^{Bg}). Figure 3A is an overlay plot of IgG^{Man9} (blue cross, "+") and IgG^{Bg} (red circle, "○"); Figure 3C is the plot of IgM^{Man9} (blue star, "*") and IgM^{Bg} (red diamond, "⋄"). ANOVA shows that this assay detected highly significant levels of IgG^{Man9} (Fig. 3B, $P < 0.0001$) and IgM^{Man9} (Fig. 3D, $P < 0.0001$) above background. Receiver operating characteristic (ROC) plots produced area under the curve (AUC) values of 0.99709 and 0.97324 for detection of IgG^{Man9} and IgM^{Man9}, respectively. Thus, this assay reached the sensitivity and specificity required to single out anti-Man9-cluster antibodies from the repertoire of human serum antibodies.

Prostatectomy Gr4/5 Cancer as "Gold Standard" for Serum Biomarker Evaluation

Our next goal was to use this ELISA to measure anti-Man9-cluster antibodies in pre-prostatectomy sera obtained from men who underwent surgery at Stanford University between 1984 and 2006 to treat PCa, and men seen in the Stanford Urology Clinic during the same period with symptoms of BPH. The latter men underwent at least two rounds of ultrasound-guided needle biopsies to rule out the presence of PCa. The former were chosen from men whose prostates had been subjected to a comprehensive histopathological review by a single pathologist [Stamey et al., 1999]. The radical pros-tatectomy specimens were sectioned at 3-mm step intervals and eight morphological variables were quantified. After correlating these morphologic variables with clinical data, Stamey and his colleagues [Stamey et al., 1999] recognized that the percent of Gr4/5 cancer in the tumor is the most significant prognostic marker predicting risk of biochemical failure (defined as serum PSA ≥ 0.07 ng/mL by the TOSOH assay on two consecutive measurements). Accordingly, we performed Nominal Logistic Fit analysis to examine whether the cohort selected for this study also illustrates such a correlation. We found that total volume of Gr4/5 and % Gr4/5 as independent classifiers for this modeling analysis produced AUC values of 0.91165 and 0.91921 for predicting biochemical recurrence, respectively (Fig. 4). Thus, the two parameters are equally effective in predicting failure or cure after prostatectomy in this cohort. This cohort is, therefore, highly valuable for evaluating serum biomarkers of aPCa and prediction of the clinical outcome after radical prostatectomy to treat PCa.

Detection of TM10-Like Anti-Man9-Cluster Autoantibodies in Men with BPH or PCa

Using the Man9-cluster ELISA to analyze the Stanford cohort, we investigated whether TM10-like antibodies are present in human circulation and whether the titers of these antitumor carbohydrate antibodies differ among men with BPH, men with cancer containing only Gr3, and men whose cancers contain different amounts of Gr4/5. In Figure 5, we analyzed 423 subjects in this cohort. These included patients with Gr3 cancer ($n = 84$), Gr4/5 cancer ($n = 204$), and the age-matched BPH controls ($n = 135$). In order to examine whether detection of anti-Man9 antibodies predicted the presence of aggressive PCa, men with Gr4/5 cancers were subgrouped into quartiles according to the volume of Gr4/5 cancer in a given subject (Figs 4 and 5).

Figure 5A shows that IgM^{Man9} was detected in all subgroups. As illustrated by the means diamonds and comparison circles in the figure and determined by the Wilcoxon nonparametric test, levels of IgM^{Man9} were not significantly different between men with BPH versus men with Gr3 cancer. However, the levels of IgM^{Man9} in certain of the subgroups of men with Gr4/5 cancer differed significantly from the BPH and Gr3 groups. Notably, the two subgroups with the largest total volumes of Gr4/5 cancer (≥3.99 cc) expressed higher levels of IgM^{Man9} than BPH ($P = 0.0012$ and 0.0149 for BPH versus Gr4/5 3.99–7.0211 cc and BPH versus Gr4/5 7.03–40.67 cc, respectively) and Gr3 ($P = 0.0130$ and 0.0835 for Gr3 versus Gr4/5 3.99–7.0211 cc and Gr3 versus Gr4/5 7.03–40.67 cc, respectively). Similarly to the IgM profile, we detected significant amounts of IgG^{Man9} in all subgroups (Fig. 5B). The levels of IgG^{Man9} in the subgroup with the largest volume of Gr4/5 cancer (≥7.03 cc) were significantly higher than those detected in men with BPH ($P = 0.0084$), Gr3 cancer ($P = 0.0064$), and other subgroups of Gr4/5 cancer ($P = 0.0140$, 0.0008, and 0.0526 for its pair with Gr4/5 < 0.91 cc, Gr4/5 0.91–3.95 cc, and Gr4/5 3.99–7.0211 cc, respectively). Results of the Wilcoxon nonparametric test for all the pairwise comparisons are shown in Table 3.

In Figure 5C and D, we examined whether Ig^{Man9} antibodies correlated with prostate weight, a parameter previously found to be strongly correlated to serum PSA levels [Stamey et al., 2004]. For this purpose, we subgrouped all cancer subjects into quartiles based on the prostate weights. Neither IgM^{Man9} (Fig. 5C) nor IgG^{Man9} (Fig. 5D) levels showed correlation to the prostate weights. We also examined correlation of antibody levels with other cancer parameters, such as the volume of nonaggressive Gr3 cancer. Unlike serum PSA values, which are positively correlated to both the Gr3 volume and prostate weight, levels of serum IgM^{Man9} and IgG^{Man9} had no correlation to these parameters (data not shown).

A significant portion of patients ($n = 259$, 61.2%) in this cohort are in the PSA “grey zone,” with PSA values <10.0 ng/mL. At these levels, PSA does not distinguish men with PCa from those with BPH with high specificity or predict risk of recurrence after surgery with high confidence [Stamey et al., 2004]. As shown by ANOVA of these data (Fig. 6 and Table 4), the performance of Ig^{Man9} signatures illustrated in Figure 5 was reproduced in this challenging population. The levels of both IgM^{Man9} and IgG^{Man9} were significantly increased in the subgroups with the larger volume Gr4/5 PCa (Fig. 6B and C). Logistic regression analysis suggests that Ig^{Man9} is highly significant in predicting the clinical outcome of men postprostatectomy. Ig^{Man9} plus PSA and PSA alone produced an AUC value of 0.72338 and 0.65221, respectively. This result suggests that Ig^{Man9} and PSA are synergistic in predicting the clinical outcome of PCa.

In Figure 7, a scatterplot matrix is used to examine the relative values of these predictors in detection of the larger volume of Gr4/5 PCa (Fig. 7A) and prediction of clinical outcome of patients (Fig. 7B). Visual inspection of the pairs of Log2-PSA, Log2-IgM^{Man9}, and Log2-IgG^{Man9} reveals clusters of red dots in the upper and right sections of the plots, which are associated with increasing values of these serum markers.

DISCUSSION

N-Glycan Cryptic Glyco-Epitopes Recognized by mAb TM10 and Human Serum IgM^{Man9} and IgG^{Man9}

The presence of Ig^{Man9} in the human circulation, initially discovered by a pilot carbohydrate microarray analysis [Wang et al., 2011], is now confirmed by a large-scale serological study of 423 subjects. This result is in striking contrast with the fact that a broad, decade-long search for induction of anti-oligomannose antibodies by HIV-1 vaccines has been unsuccessful [Ni et al., 2006; Wang, 2006; Barouch, 2008; Willyard, 2010]. We asked, therefore, whether and how the tumor-associated oligomannosyl antigens differ from the 2G12-positive HIV-1-carbohydrates in their structural characteristics. MAb TM10 and 2G12 have served as key reagents to probe the similarities and differences between the HIV-1 carbohydrates recognized by 2G12 and the tumor-associated TM10-carbohydrates.

In Figure 1, we characterized the binding specificities of TM10 and 2G12 by carbohydrate microarrays, which contain a panel of mannose-clusters of different structural characteristics. As shown in Figure 1C and D, the two mAbs differ in binding activity with the oligomannosyl antigens of different cluster configurations. 2G12 is specific for the high-density Man9-clusters presented by [(Man9)4]n-KLH, which mimics the HIV-1 virion-presenting of the oligomannose antigens; TM10 is, however, similarly reactive with the three Man9-conjugates spotted in the same array without selectivity. In an antigen-specific ELISA, we further demonstrated that TM10 binds to (Man9)n-BSA but not to (Man5)n-BSA. As illustrated in Figure 2A, (Man9)n-BSA and (Man5)n-BSA differ in their terminal mannosyl moieties. The former displays Manα1,2Man-moieties; the latter expresses no terminal Manα1,2Man-moiety but presents Manα1,3Man and Manα1,6Man moieties at its terminals. Thus, TM10 recognizes the terminal Manα1,2Man-glyco-epitopes that are also bound by 2G12. Apparently, the tumor-associated TM10-antigen differs from the HIV-1-specific 2G12-antigen only by its Man9-cluster configuration. Further structural analysis, such as crystallographic investigation of TM10 binding sites, may lead to a better understanding of TM10-binding of the tumor-specific Man9-clusters.

Detection of Serum Ig^{Man9} Significantly Predicts the Presence of Aggressive Cancers

With the Stanford reference set, it is possible to examine whether a serum marker is correlated to the key surgical parameters of PCa severity, such as presence of high % and large volume Gr4/5 cancer, and whether detection of such a marker predicts the clinical outcome of the disease. To address these questions, we have performed further statistical analysis to estimate the effectiveness of Ig^{Man9} in detection of the large volume and high % Gr4/5 cancers in PCa patients. First, we performed a Least Squares Fit analysis to test IgM^{Man9} and IgG^{Man9} for prediction of either large volume or high % Gr4/5, independently. For predicting % Gr4/5, IgM^{Man9} statistics are $P < 0.0001$, RSquare (RSq) 0.04, and root-mean-square error (RMSE) 33.614; the IgG^{Man9} values are $P = 0.0036$; RSq 0.02, and RMSE 33.95. When volume of G4/5 cancer is targeted for this modeling analysis, IgM^{Man9} statistics are $P = 0.066$, RSq 0.01, and RMSE 5.1788; IgG^{Man9} values are $P = 0.0008$; RSq 0.03, and RMSE 5.1318. Thus, IgM^{Man9} and IgG^{Man9} significantly predict the % or volume

of G4/5 cancer. The degrees of significance of each parameter, as estimated by RSq values, varied among parameters.

Next, we examined whether IgM^{Man9} and IgG^{Man9} improve the predictive effects in synergy with PSA, which is predictive of the cancer volume or prostate weight. We observed that PSA plus Ig^{Man9} (IgM^{Man9} and IgG^{Man9}) are highly significant in predicting the % or volume of G4/5 cancer in this cohort. For detection of % Gr4/5 cancer, the RSq values of PSA and PSA plus Ig^{Man9} are 0.07 and 0.12, respectively. That means the two markers in combination increased the weight of influence from 7% by PSA alone to 12% of the total variation. When the volume of Gr4/5 was calculated, RSq values of PSA and PSA plus Ig^{Man9} are 0.24 and 0.28, which are weighted 24% and 28%, respectively. In Figure 7, the red dots of high-volume Gr4/5 (>50%) (Fig. 7A) or clinical failure (Fig. 7B) were clustered in the upper and right areas in association with the increasing values of Log_2PSA and Log_2IgM^{Man9} or Log_2PSA and Log_2IgG^{Man9}.

Ig^{Man9} and PSA Illustrate Synergistic Effects in Predicting Clinical Outcome Post-radical Prostatectomy

Prostate needle biopsy (PNBx) is another principal clinical examination that is currently employed to risk stratify newly diagnosed PCa patients (http://www.nccn.org). In the United States, ~90% of patients are diagnosed with clinical stage T1c, which is characterized by an elevated PSA but normal digital rectal exam with a PNBx revealing malignancy. Most PCa is diagnosed in the setting of a low PSA (<10 ng/mL) and no palpable prostate mass (cT1c). In these cases, the PNBx Gleason score, that is, sum of the two most prominent Gleason grades, is the predominant factor used to render clinical decision of either aPCa or iPCa. However, there are many cases of under- and overgrading in PNBx as compared with the radical prostatectomy Gleason scores [D'Amico et al., 1999; Grossfeld et al., 2001; Isariyawongse et al., 2008]. Given a recent report on 2,963 cases of PCa receiving radical prostatectomy in Duke University [Isariyawongse et al., 2008], the rates of discrepancies between the diagnostic and the pathologic Gleason sums are substantially high. Overall, 55.8% of the diagnostic Gleason sums differed from those on final surgical pathology, including the undergraded diagnosis in 41.2% of cases and the over-graded in 12.8% of cases.

It is understood that neither serum PSA levels nor PNBx correctly reveal the volume or grade of cancer in the prostate [Noguchi et al., 2001; King et al., 2004]. Measurement of the volume or % of Gr4/5 PCa in a subject can only be achieved after radical prostatectomy. Thus, identification of Ig^{Man9} as a predictor of the large volume/high percentage of Gr4/5 PCa, a class of well-defined aggressive PCa, especially in the population of low PSA (<10 ng/mL), is of high significance. Nevertheless, the sum of the prognostic power of the two serum markers as calculated in Figure 6 (~72%) remains significantly lower than the ~91% accuracy as estimated by the ROC curves when surgical % or volume of Gr4/5 cancer serves as the predictor of clinical status (Fig. 4B and C). A better performance of PCa prognosis and differential diagnosis may be achieved by integrating the diagnostic potential of these anti-glycan antibodies and other serum markers, such as autoantibodies to PCa-specific proteins [Massoner et al., 2012], O-glycopeptides [Wandall et al., 2010], and the xeno-

autoantibodies elicited by the dietary nonhuman sialic acid Neu5Gc [Padler-Karavani et al., 2011].

It is worthwhile to note that we have observed a profile of IgM^{Man9} and IgG^{Man9} reactivities in the Stan-ford cohort that is strongly associated with the progression of Gr4/5 cancers (Figs 5 and 6). In the subgroups with the smaller volume Gr4/5 cancers, that is, subgroups 3 (1–25% quartile) and 4 (26–50% quartile), serum IgM^{Man9} levels were decreased as compared with those detected in BPH and Gr3 cancers. By contrast, they were significantly increased in the larger volume Gr4/5 cancers, including subgroups 5 (51–75% quartile) and 6 (76–100% quartile). The serum IgG^{Man9} response was found, however, to occur subsequently in the subgroup 6 of the worst form of aggressive PCa. The kinetics of this antibody responding profile, as observed in a patient population, implicates the active involvement of both the innate and the acquired humoral immunities in the surveillance of the disease progression, which remains to be further investigated.

Acknowledgments

We acknowledge Dr. Leonore A. Herzenberg for many helpful discussions. Dr. Thomas E Newsom-Davis of Imperial College London for mAb TM10; the NIH AIDS Research and Reference Reagent Program for mAb 2G12; and the Kabat Collection of Carbohydrate Antigens and Antibodies at SRI International for glyco-conjugates IM3-BSA and IM6-BSA used in this study.

The project described was supported by grant number U01CA128416 and U01CA128416-S2 to D. Wang from the NCI/NIH and grant number R01 AI067111 to L-X. Wang from NIAID/NIH. The content is solely the responsibility of the authors and does not necessarily represent the official views of the National Institutes of Health.

References

Bach PB, Elkin EB, Pastorino U, Kattan MW, Mushlin AI, Begg CB, Parkin DM. Benchmarking lung cancer mortality rates in current and former smokers. Chest. 2004; 126:1742–1749. [PubMed: 15596668]

Barouch DH. Challenges in the development of an HIV-1 vaccine. Nature. 2008; 455:613–619. [PubMed: 18833271]

D'Amico AV, Renshaw AA, Arsenault L, Schultz D, Richie JP. Clinical predictors of upgrading to Gleason grade 4 or 5 disease at radical prostatectomy: potential implications for patient selection for radiation and androgen suppression therapy. Int J Radiat Oncol Biol Phys. 1999; 45:841–846. [PubMed: 10571187]

DeSantis C, Howlader N, Cronin KA, Jemal A. Breast cancer incidence rates in U.S. women are no longer declining. Cancer Epidemiol Biomarkers Prev. 2011a; 20:733–739. [PubMed: 21357727]

DeSantis C, Siegel R, Bandi P, Jemal A. Breast cancer statistics, 2011. CA Cancer J Clin. 2011b; 61:409–418. [PubMed: 21969133]

Goldstein IJ, Hollerman CE, Smith EE. Protein-carbohydrate interaction. II. Inhibition studies on the interaction of concanavalin a with polysaccharides. Biochemistry. 1965; 4:876–883. [PubMed: 14337704]

Grossfeld GD, Chang JJ, Broering JM, Li YP, Lubeck DP, Flanders SC, Carroll PR. Under staging and under grading in a contemporary series of patients undergoing radical prostatectomy: results from the Cancer of the Prostate Strategic Urologic Research Endeavor database. J Urol. 2001; 165:851–856. [PubMed: 11176485]

Isariyawongse BK, Sun L, Banez LL, Robertson C, Polascik TJ, Maloney K, Donatucci C, Albala D, Mouraviev V, Madden JF, et al. Significant discrepancies between diagnostic and pathologic Gleason sums in prostate cancer: the predictive role of age and prostate-specific antigen. Urology. 2008; 72:882–886. [PubMed: 18384857]

Kabat EA, Nickerson KG, Liao J, Grossbard L, Osserman EF, Glickman E, Chess L, Robbins JB, Schneerson R, Yang YH. A human monoclonal macroglobulin with specificity for alpha(2–8)-linked poly-N-acetyl neuraminic acid, the capsular polysaccharide of group B meningococci and Escherichia coli K1, which crossreacts with polynucleotides and with denatured DNA. J Exp Med. 1986; 164:642–654. [PubMed: 3088209]

King CR, McNeal JE, Gill H, Presti JC Jr. Extended prostate biopsy scheme improves reliability of Gleason grading: implications for radiotherapy patients. Int J Radiat Oncol Biol Phys. 2004; 59:386–391. [PubMed: 15145152]

Lange T, Ullrich S, Müller I, Nentwich MF, Stuebke K, Feldhaus S, Knies C, Hellwinkel OJC, Vessella RL, Abramjuk C, et al. A Human prostate cancer in a clinically relevant Xenograft Mouse Model: identification of β(1,6)-branched oligosaccharides as a marker of tumor progression. Clinical Cancer Res. 2012; 18:1364–1373. Published Online First on January 18, 2012. 10.1158/1078-0432.CCR-11-2900 [PubMed: 22261809]

Li H, Wang LX. Design and synthesis of a template-assembled oligomannose cluster as an epitope mimic for human HIV-neutralizing antibody 2G12. Org Biomol Chem. 2004; 2:483–488. [PubMed: 14770226]

Massoner P, Lueking A, Goehler H, Hopfner A, Kowald A, Kugler KG, Amersdorfer P, Horninger W, Bartsch G, Schulz-Knappe P, et al. Serum-autoantibodies for discovery of prostate cancer specific biomarkers. Prostate. 2012; 72:427–436. [PubMed: 22012634]

Newsom-Davis TE, Wang D, Steinman L, Chen PF, Wang LX, Simon AK, Screaton GR. Enhanced immune recognition of cryptic glycan markers in human tumors. Cancer Res. 2009; 69:2018–2025. [PubMed: 19223535]

Ni J, Song H, Wang Y, Stamatos NM, Wang LX. Toward a carbohydrate-based HIV-1 vaccine: synthesis and immunological studies of oligomannose-containing glycoconjugates. Bioconjug Chem. 2006; 17:493–500. [PubMed: 16536482]

Noguchi M, Stamey TA, McNeal JE, Yemoto CM. Relationship between systematic biopsies and histological features of 222 radical prostatectomy specimens: lack of prediction of tumor significance for men with nonpalpable prostate cancer. J Urol. 2001; 166:104–109. discussion 109–110. [PubMed: 11435833]

Padler-Karavani V, Hurtado-Ziola N, Pu M, Yu H, Huang S, Muthana S, Chokhawala HA, Cao H, Secrest P, Friedmann-Morvinski D, et al. Human xeno-autoantibodies against a non-human sialic acid serve as novel serum biomarkers and immunotherapeutics in cancer. Cancer Res. 2011; 71:3352–3363. [PubMed: 21505105]

Ries LA. Influence of extent of disease, histology, and demographic factors on lung cancer survival in the SEER population-based data. Semin Surg Oncol. 1994; 10:21–30. [PubMed: 8115783]

Sanders RW, Venturi M, Schiffner L, Kalyanaraman R, Katinger H, Lloyd KO, Kwong PD, Moore JP. The mannose-dependent epitope for neutralizing antibody 2G12 on human immunodeficiency virus type 1 glycoprotein gp120. J Virol. 2002; 76:7293–7305. [PubMed: 12072528]

Scanlan CN, Pantophlet R, Wormald MR, Ollmann Saphire E, Stanfield R, Wilson IA, Katinger H, Dwek RA, Rudd PM, Burton DR. The broadly neutralizing anti-human immunodeficiency virus type 1 antibody 2G12 recognizes a cluster of alpha1-->2 mannose residues on the outer face of gp120. J Virol. 2002; 76:7306–7321. [PubMed: 12072529]

Stamey TA, Freiha FS, McNeal JE, Redwine EA, Whittemore AS, Schmid HP. Localized prostate cancer. Relationship of tumor volume to clinical significance for treatment of prostate cancer. Cancer. 1993; 71(3 Suppl):933–938. [PubMed: 7679045]

Stamey TA, McNeal JE, Yemoto CM, Sigal BM, Johnstone IM. Biological determinants of cancer progression in men with prostate cancer. JAMA. 1999; 281:1395–1400. [PubMed: 10217055]

Stamey TA, Caldwell M, McNeal JE, Nolley R, Hemenez M, Downs J. The prostate specific antigen era in the United States is over for prostate cancer: what happened in the last 20 years? J Urol. 2004; 172(4 Pt 1):1297–1301. [PubMed: 15371827]

Trkola A, Purtscher M, Muster T, Ballaun C, Buchacher A, Sullivan N, Srinivasan K, Sodroski J, Moore JP, Katinger H. Human monoclonal antibody 2G12 defines a distinctive neutralization epitope on the gp120 glycoprotein of human immunodeficiency virus type 1. J Virol. 1996; 70:1100–1108. [PubMed: 8551569]

Wandall HH, Blixt O, Tarp MA, Pedersen JW, Bennett EP, Mandel U, Ragupathi G, Livingston PO, Hollingsworth MA, Taylor-Papadimitriou J, et al. Cancer biomarkers defined by autoantibody signatures to aberrant O-glycopeptide epitopes. Cancer Res. 2010; 70:1306–1313. [PubMed: 20124478]

Wang D. N-glycan cryptic antigens as active immunological targets in prostate cancer patients. J Proteomics Bioinform. 2012; 5:090–095.

Wang, D.; Herzenberg, LA. The Board of Trustees of the Leland Stanford Junior University. Glycan markers and auto-antibody signatures in HIV-1 and HIV-1-associated malignancies. Patent application No. 20110177090. 2011. Files Jan 19 2011

Wang D, Liu S, Trummer BJ, Deng C, Wang A. Carbohydrate microarrays for the recognition of cross-reactive molecular markers of microbes and host cells. Nat Biotechnol. 2002; 20:275–281. [PubMed: 11875429]

Wang, D.; Herzenberg, LA.; Peehl, D.; Herzenberg, LA. Prostate cancer glycan markers and auto-antibody signatures. U.S. Patent No. 7,981,625. 2011 Jul 19. 2011

Wang LX. Toward oligosaccharide- and glycopeptide-based HIV vaccines. Curr Opin Drug Discov Devel. 2006; 9:194–206.

Wang LX, Ni J, Singh S, Li H. Binding of high-mannose-type oligosaccharides and synthetic oligomannose clusters to human antibody 2G12: implications for HIV-1 vaccine design. Chem Biol. 2004; 11:127–134. [PubMed: 15113002]

Willyard C. Tiny steps towards an HIV vaccine. Nature. 2010; 466:S8. [PubMed: 20631706]

Zopf DA, Tsai CM, Goinsburg V. Carbohydrate antigens: coupling fo oligosaccharide-phenethylamine derivatives to edestin by diazotization and characterization of antibody specificity by radio-immunoassay. Methods Enzymol. 1978; 50:163–169. [PubMed: 351327]

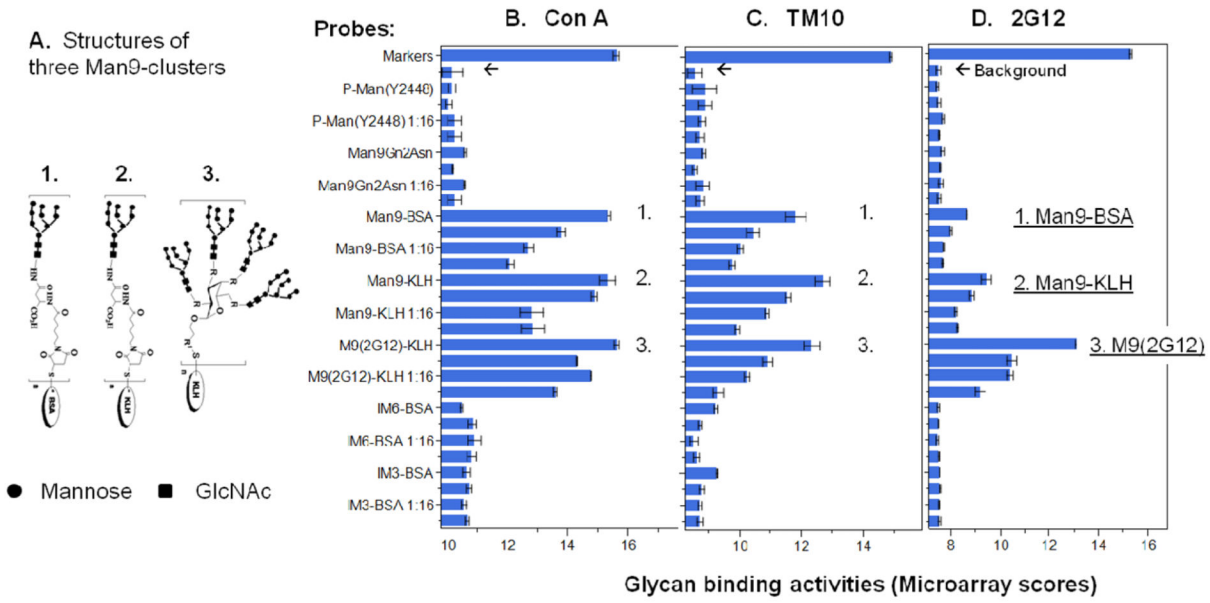

Fig. 1.

Carbohydrate microarrays identify tumor-associated oligomannosyl antigens that differ from the 2G12-specific HIV-1 carbohydrates by the Man9-cluster configuration. The glycan-binding activities of antibody/lectin are shown as microarray scores, which are the log2-transformed mean microarray values of triplicate detections. Panel (**A**) illustrates the structures of three Man9-conjugates: (1) Man9-BSA, (2) Man9-KLH, and (3) M9(2G12). The latter stands for [(Man9)4]n-KLH in the figure. The binding profiles of ConA, TM10, and 2G12 are shown as overlay plots in panels (**B**), (**C**), and (**D**), respectively. The microarray dataset of this figure is shown in Table 2. [Color figure can be viewed in the online issue which is available at wileyonlinelibrary.com]

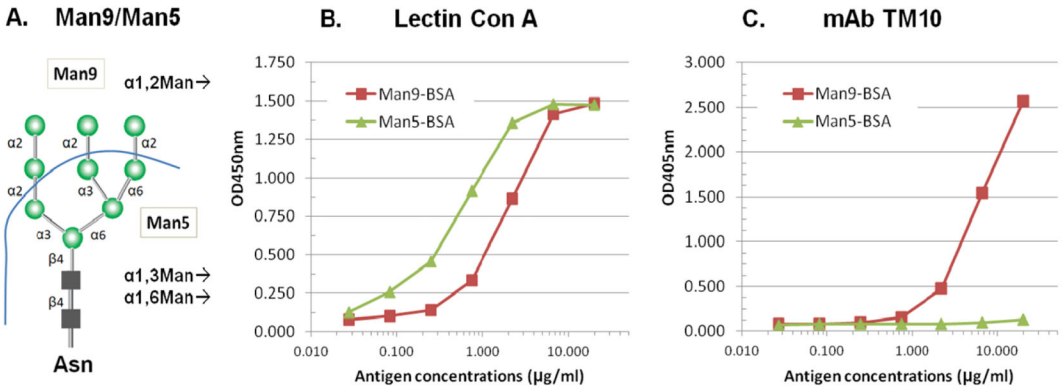

Fig. 2.

(Man9)n-BSA but not (Man5)n-BSA displays the tumor-specific TM10-glyco-epitopes in an ELISA. (**A**) Schematic of Man9 and Man5 and their terminal nonreducing end epitopes; (**B**) Con A-binding curves: biotinylated Con A was applied at 1 μg/mL on ELISA plates coated with either (Man9)n-BSA or (Man5)n-BSA. The bound Con A was revealed by staining the ELISA plates with Streptavidin-HRP; and (**C**) TM10-binding curves: TM10 (IgM) culture supernatant was applied at 1:5 dilutions and the antigen-captured antibody was quantified by an anti-murine IgM-AP conjugate. The binding curves shown here are representative results of multiple assays. AP, alkaline phosphatase; HRP, horseradish peroxidase; ELISA, enzyme-linked immunosorbent assay. [Color figure can be viewed in the online issue which is available at wileyonlinelibrary.com]

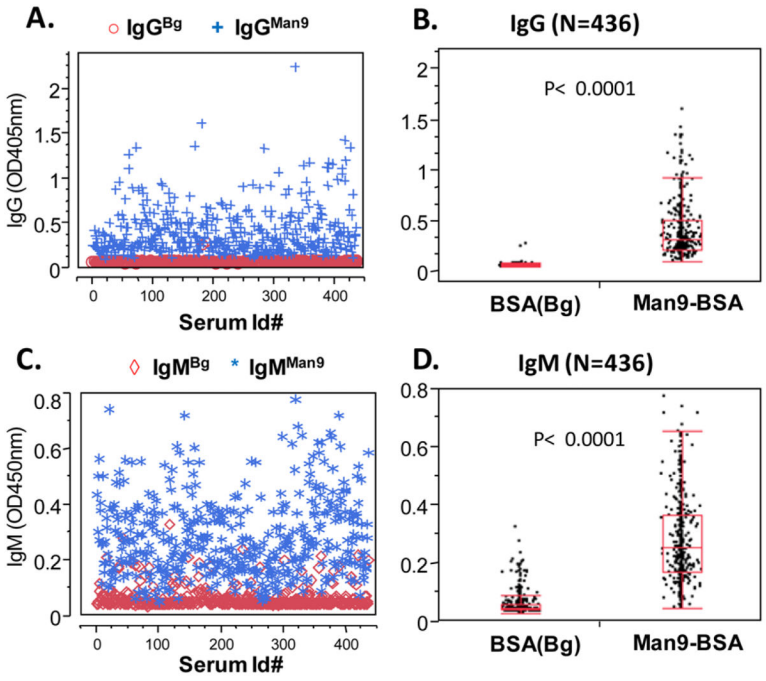

Fig. 3.

An ELISA for highly sensitive detection of serum IgM^{Man9} and IgG^{Man9} in human population. (**A**) and (**B**) IgG; (**C**) and (**D**) IgM; (**A**) and (**C**) ELISA values; (**B**) and (**D**) ANOVA between background (BSA) and anti-Man9 antibodies. ELISA, enzyme-linked immunosorbent assay. [Color figure can be viewed in the online issue which is available at wileyonlinelibrary.com]

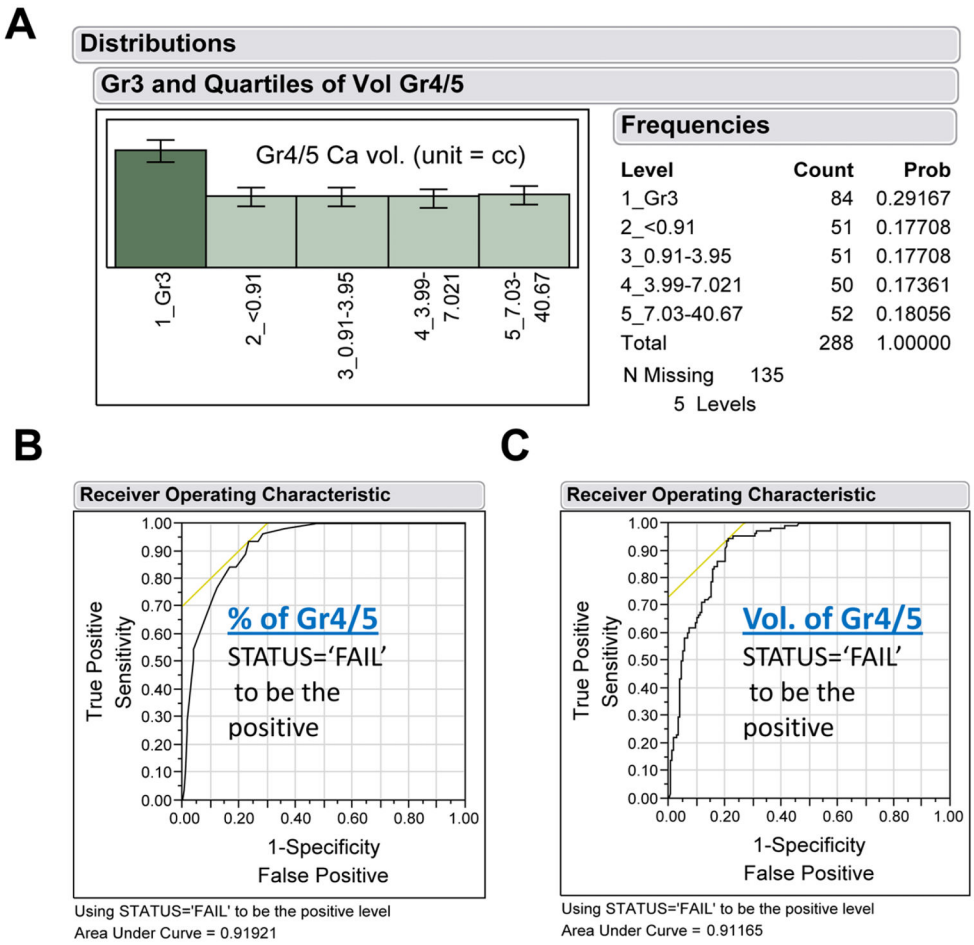

Fig. 4.

Surgical % or volume of Gleason grades as "gold standard" for evaluation of serum biomarkers of prostate cancer. **A**) Subgroup distribution of 288 PCa subjects; **B**) Nominal Logistic Fit of % Gr4/5 for predicting clinical outcome, either Failure or Cure, post-radical prostatectomy; and **C**) Nominal Logistic Fit of total volume of Gr4/5 for predicting clinical outcome. The failure status was determined by recurrence of the cancer as measured by serum PSA levels. [Color figure can be viewed in the online issue which is available at wileyonlinelibrary.com]

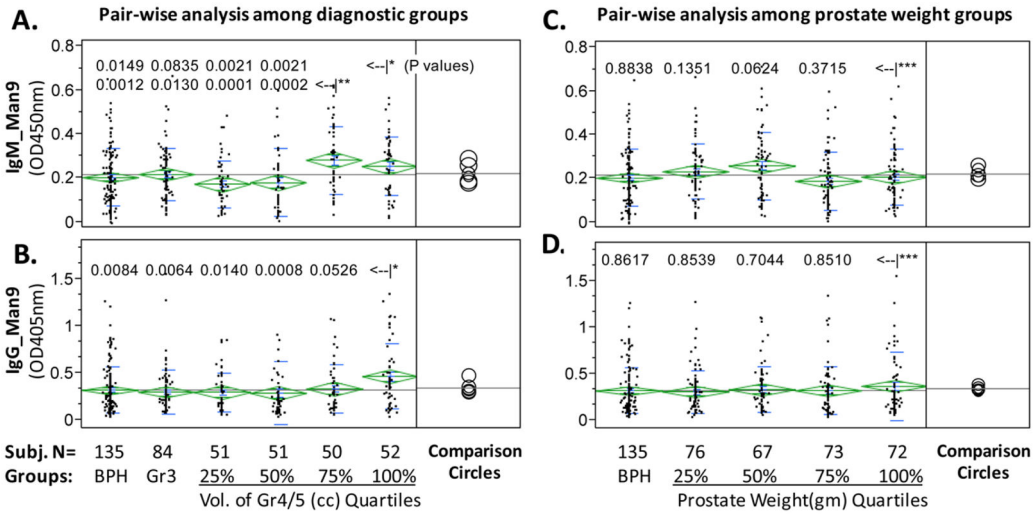

Fig. 5.

Antigen-specific ELISA detected anti-Man9 autoantibodies (Ig^{Man9}) in the Stanford Cohort. ELISA results shown here were background subtracted antigen-specific OD values. One-way analysis was performed to compare group means, which are shown as the means diamonds. The comparison circles appear to the right of the means diamonds to assist visual inspection of differences among means. The more the circles intersect, the less the significance of difference. A nonparametric statistical test (Wilcoxon rank-sum method) was applied to determine the significance of differences among subgroups (Table 3). In panels (**A**) and (**B**), the Gr4/5 group was further divided into quartiles based on the total volume of Gr4/5 cancer in a given subject. In panels (**C**) and (**D**), all cancer subjects were subgrouped based on prostate weights. *P*-values for pairwise comparison between the 3rd (<–|*) and 4th quartile (<–|**) of Gr4/5 and other groups (panels **A** and **B**), or between the 5th prostate weight group and other groups (<–|***) (panels **C** and **D**), were listed with corresponding group in comparison. The datasets presented here are representative of three large-scale serological studies with similar design and outcome. ELISA, enzyme-linked immunosorbent assay. [Color figure can be viewed in the online issue which is available at wileyonlinelibrary.com]

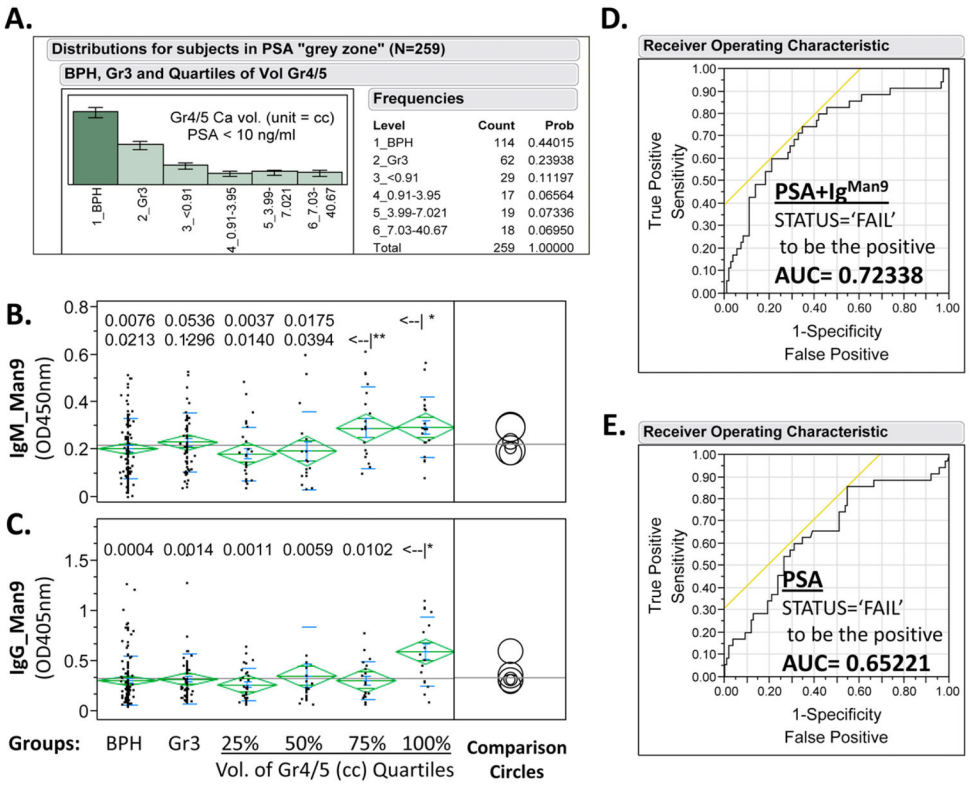

Fig. 6.

Ig^{Man9} and PSA illustrate synergistic effects in prediction of clinical status. (**A**) Subgroup distribution of 259 subjects with PSA cutoff value of 10 ng/mL; (**B**) and (**C**) One-way analysis of IgG^{Man9} or IgM^{Man9} by BPH, Gr3, and the Gr4/5 quartile subgroups. A nonparametric statistical test (Wilcoxon rank-sum method) was applied to calculate the significance of differences among subgroups. *P*-values for pairwise comparison between the 3rd (<–|*) or 4th quartile (<–|**) of Gr4/5 and other groups (panels **B** and **C**) were listed; results of all pairs are shown in Table 4. (**D**) Nominal Logistic Fit of PSA, IgG^{Man9}, and IgM^{Man9} for predicting clinical outcome, either Failure or Cure, postradical prostatectomy; and (**E**) Nominal Logistic Fit of PSA for predicting clinical outcome, either Failure or Cure, postradical prostatectomy. The failure status was determined by recurrence of the cancer as measured by serum PSA levels. ROC plots produced AUC values of 0.65221, 0.63766, 0.55390, and 0.72338 for PSA, IgG^{Man9}, IgM^{Man9}, and a combination of PSA, IgG^{Man9}, and IgM^{Man9}, respectively. AUC, area under the curve; BPH, benign prostatic hyperplasia; ROC, receiver operating characteristic. [Color figure can be viewed in the online issue which is available at wileyonlinelibrary.com]

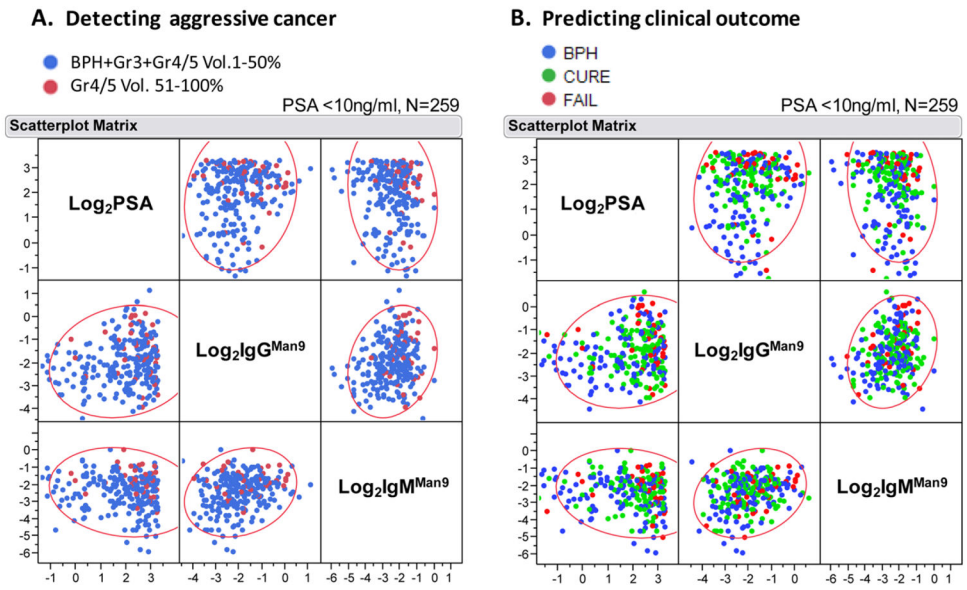

Fig. 7.

Multivariate plots of Log_2PSA, Log_2IgM^{Man9}, and Log_2IgG^{Man9} in a PSA gray zone population (n = 259). Each dot in the Scatterplot Matrix represents one subject; the color of dot classifies subject groups as marked in each graph. (**A**) Distribution of Gr4/5 Vol. 51–100% (colored in red) among other groups, including BPH, Gr3, or Gr4/5 Vol. 1–50% (colored in blue); (**B**) distribution of BPH (blue), clinical Cure (green); and clinical Failure (red) postradical prostatectomy. BPH, benign prostatic hyperplasia.

TABLE 1

Carbohydrate Antigens and control Reagents Utilized in Figures 1 and 2

Probes	Description	Laboratory or commercial origins	References
Spotting markers	Streptavidin-Cy3, -Cy5 and -FITC	Amashan Pharmacia (Piscataway, NJ)	This report
Man5-BSA	(Man5GlcNAc2Asn)n-BSA	From Prof. Lai-Xi Wang (University of Maryland)	This report
Man9-BSA	(Man9GlcNAc2Asn)n-BSA	From Prof. Lai-Xi Wang (University of Maryland)	This report
Man9Gn2Asn	Man9GlcNAc2Asn	From Prof. Lai-Xi Wang (University of Maryland)	Wang et al., 2004
Man9-KLH	(Man9GlcNAc2Asn)n-KLH	From Prof. Lai-Xi Wang (University of Maryland)	Ni et al., 2006
M9(2G12)-KLH	[(Man9GlcNAc2Asn)4]n-KLH, mAb 2G12 positive	From Prof. Lai-Xi Wang (University of Maryland)	Ni et al., 2006
P-Man(Y2448)	Phosphomannan from Pichia (Ha nsenula)holstii NRRL B-2448	Northern Regional research laboratory (Peoria, IL)	Kabat et al., 1986
IM3-BSA	Isomaltotriose-BSA	From the late Prof. Elvin A. Kabat (Columbia University)	Zopf et al., 1978
IM6-BSA	Isomaltohexaose-BSA	From the late Prof. Elvin A. Kabat (Columbia University)	Zopf et al., 1978

TABLE 2

Dataset from a Carbohydrate Microarray Analysis Illustrated in Figure 1

Probes*	ConA_Mean†	ConA_StDEV	ConA_P Value	TM10_Mean	TM10_StDEV	TM10_P Value	2G12_Mean	2G12_StDEV	2G12_P Value
Markers	15.62260	0.08803		14.87944	0.03441		15.29192	0.04377	
Bg	10.15045	0.35743		8.57881	0.22869		7.47497	0.07922	
P-Man(Y2448)	10.14444	0.10068	0.940820863	8.89631	0.38837	0.291392061	7.42838	0.05436	0.271620451
P-Man(Y2448) 1:4	10.02619	0.11502	0.198823146	8.89071	0.22099	0.126203928	7.49059	0.07411	0.75417976
P-Man(Y2448) 1:16	10.22374	0.22526	0.640614989	8.79379	0.10916	0.051393781	7.66249	0.04541	0.008628676
P-Man(Y2448) 1:64	10.21577	0.23261	0.684575226	8.73164	0.11542	0.129350814	7.51277	0.03622	0.2012504
Man9Gn2Asn	10.56420	0.03388	3.10365E-09	8.84279	0.05150	0.000186025	7.63270	0.08081	0.069635964
Man9Gn2Asn 1:4	10.17306	0.02918	0.67885688	8.57376	0.07029	0.926499249	7.56456	0.03088	0.013694735
Man9Gn2Asn 1:16	10.54928	0.02807	2.44692E-09	8.82917	0.20845	0.165188048	7.56701	0.11018	0.283223321
Man9Gn2Asn 1:64	10.21524	0.22238	0.674811757	8.74372	0.12149	0.124014225	7.51466	0.06714	0.415769869
Man9-BSA	15.37738	0.04432	2.68836E-38	11.80805	0.34211	0.003009395	8.64861	0.01364	6.62876E-23
Man9-BSA 1:4	13.77593	0.13463	1.9426E-06	10.44396	0.20741	0.002335723	7.98646	0.03816	0.000159817
Man9-BSA 1:16	12.69489	0.15874	5.61045E-05	10.03899	0.08779	1.65465E-05	7.68872	0.02239	1.33477E-05
Man9-BSA 1:64	12.07279	0.13098	1.84638E-05	9.77254	0.09933	0.000133201	7.64338	0.04537	0.011461192
Man9-KLH	15.34345	0.26847	0.000275556	12.69134	0.23369	0.000585963	9.42776	0.20184	0.003289325
Man9-KLH 1:4	14.88474	0.09853	3.43586E-10	11.56674	0.10104	6.52014E-06	8.83664	0.08059	0.000638523
Man9-KLH 1:16	12.79414	0.39658	0.005414037	10.88833	0.06345	2.40296E-09	8.18735	0.05987	0.00092076
Man9-KLH 1:64	12.83746	0.37199	0.00434454	9.93017	0.06795	3.47497E-07	8.25379	0.04418	0.000136099
M9(2G12)-KLH	15.61902	0.07991	1.03991E-14	12.33137	0.26252	0.001048246	13.15391	0.10919	7.64838E-05
M9(2G12)-KLH 1:4	14.31340	0.02031	3.59841E-53	10.91850	0.16253	0.000504444	10.46516	0.19371	0.001263399
M9(2G12)-KLH 1:16	14.78672	0.01339	2.01736E-55	10.25366	0.09705	3.18249E-05	10.39027	0.11542	0.000371526
M9(2G12)-KLH 1:64	13.58205	0.04742	5.36118E-30	9.32447	0.15719	0.007707144	9.18056	0.20245	0.004355371
IM3-BSA	10.61543	0.12902	0.005480001	9.28675	0.02911	6.10235E-18	7.52614	0.01194	0.000950827
IM3-BSA 1:4	10.71662	0.09804	0.000213755	8.79156	0.08706	0.023421608	7.54167	0.01782	0.001711139
IM3-BSA 1:16	10.54305	0.08291	0.000367012	8.72945	0.05673	0.012339767	7.52081	0.02394	0.04617645
IM3-BSA 1:64	10.64495	0.07517	1.69228E-05	8.72927	0.09442	0.082587341	7.50464	0.04693	0.392809306
IM6-BSA	10.43775	0.03868	1.04823E-05	9.23601	0.05874	1.62475E-06	7.46717	0.04346	0.796089443
IM6-BSA 1:4	10.82836	0.13053	0.00134988	8.73535	0.04603	0.003178209	7.48380	0.00806	0.478895723

Probes*	ConA_Mean†	ConA_StDEV	ConA_P Value	TM10_Mean	TM10_StDEV	TM10_P Value	2G12_Mean	2G12_StDEV	2G12_P Value
IM6-BSA 1:16	10.88267	0.21738	0.015840704	8.54127	0.13638	0.692285058	7.43688	0.04761	0.297995151
IM6-BSA 1:64	10.79073	0.14876	0.004058511	8.62936	0.10220	0.502602184	7.49967	0.02777	0.270985768

*Probe's initial spotting concentration at ng/mL: P-Man 0.25, Man9Gn2Asn 1.0, Man9-BSA 0.5, Man9-KLH 0.5, M9(2G12)-KLH 0.5, IM3-BSA 0.25, IM6-BSA 0.25.

†Mean, StDEV and *t*-test: The log2-transform ed microarray values from triplicate spots for each antigen were included in a statistic analysis. *t*-Test was performed to examine the differences of significance between each probe and Bg (background), which is background reading of 48 "None" spots in the same microarray image.

IM, isomaltotriose; M9(2G12), [(Man9)4]n; P-Man, phophomannan.

TABLE 3

Results of One-Way ANOVA of IgM_M9-Bg (A) or IgG_M9-Bg (B) by BPH, Gr3, and the Quartile Subgroups of Gr4/5 (Levels 3–6)

Level	- Level	Score mean difference	Std Err Dif	*Z*	*P*-value	Hodges–Lehmann	Lower CL	Upper CL
A. IgM_M9-Bg								
5_3.99-7.021	1_BPH	28.6270	8.864991	3.22922	0.0012*	0.079500	0.032000	0.124500
5_3.99-7.021	3_<0.91	22.6953	5.830983	3.89219	<.0001*	0.105250	0.054000	0.158500
5_3.99-7.021	4_0.91-3.95	21.9427	5.831085	3.76306	0.0002*	0.111000	0.055000	0.166500
6_7.03-40.67	1_BPH	21.5103	8.833943	2.43496	0.0149*	0.053000	0.011000	0.099000
6_7.03-40.67	3_<0.91	18.0988	5.887973	3.07386	0.0021*	0.083000	0.031000	0.133000
6_7.03-40.67	4_0.91-3.95	18.0794	5.887973	3.07056	0.0021*	0.082250	0.037000	0.142000
5_3.99-7.021	2_Gr3	17.2286	6.935038	2.48428	0.0130*	0.062000	0.014000	0.110500
6_7.03-40.67	2_Gr3	12.0339	6.952804	1.73080	0.0835	0.038250	−0.006000	0.082333
2_Gr3	1_BPH	9.2698	8.805464	1.05274	0.2925	0.016500	−0.014333	0.049000
4_0.91-3.95	3_<0.91	−3.0980	5.859233	−0.52874	0.5970	−0.011000	−0.051000	0.032000
6_7.03-40.67	5_3.99-7.021	−5.0019	5.860377	−0.85352	0.3934	−0.027000	−0.084000	0.033000
3_<0.91	1_BPH	−10.9007	8.848835	−1.23187	0.2180	−0.025000	−0.062500	0.013000
4_0.91-3.95	1_BPH	−15.0880	8.848810	−1.70509	0.0882	−0.032500	−0.072500	0.005000
3_<0.91	2_Gr3	−15.8824	6.943464	−2.28738	0.0222*	−0.043000	−0.082000	−0.006500
4_0.91-3.95	2_Gr3	−17.6471	6.943481	−2.54153	0.0110*	−0.054000	−0.093000	−0.013000
B. IgG_M9-Bg								
6_7.03-40.67	1_BPH	23.2684	8.833987	2.63397	0.0084*	0.103750	0.024000	0.1930000
6_7.03-40.67	4_0.91-3.95	19.8077	5.888005	3.36408	0.0008*	0.152667	0.056000	0.2540000
6_7.03-40.67	2_Gr3	18.9460	6.952813	2.72494	0.0064*	0.114000	0.028000	0.2000000
6_7.03-40.67	3_<0.91	14.4674	5.887892	2.45714	0.0140*	0.113000	0.021000	0.2163333
6_7.03-40.67	5_3.99-7.021	11.3573	5.860509	1.93794	0.0526	0.091000	−0.002667	0.2040000
5_3.99-7.021	4_0.91-3.95	10.2782	5.831085	1.76266	0.0780	0.050000	−0.007000	0.1190000
5_3.99-7.021	2_Gr3	2.3450	6.935046	0.33814	0.7353	0.011000	−0.047000	0.0710000
5_3.99-7.021	1_BPH	2.2474	8.865020	0.25351	0.7999	0.007000	−0.046500	0.0650000
5_3.99-7.021	3_<0.91	1.9012	5.831034	0.32604	0.7444	0.013500	−0.049000	0.0880000
2_Gr3	1_BPH	0.0000	8.805469	0.00000	1.0000	0.000000	−0.044000	0.0410000
3_<0.91	2_Gr3	−1.4811	6.943414	−0.21331	0.8311	−0.005500	−0.058000	0.0550000

Level	- Level	Score mean difference	Std Err Dif	*Z*	*P*-value	Hodges–Lehmann	Lower CL	Upper CL
3_<0.91	1_BPH	−2.3503	8.848806	−0.26561	0.7905	−0.007000	−0.060000	0.0460000
4_0.91-3.95	3_<0.91	−7.5490	5.859250	−1.28839	0.1976	−0.038000	−0.099500	0.0210000
4_0.91-3.95	2_Gr3	−12.5578	6.943507	−1.80856	0.0705	−0.043000	−0.095000	0.0040000
4_0.91-3.95	1_BPH	−15.7634	8.848831	−1.78141	0.0748	−0.043000	−0.093000	0.0040000

A nonparametric statistical test (Wilcoxon rank-sum method) was applied to calculate the significance of differences among subgroups. q* 1.95996, Alpha 0.05.

TABLE 4

Results of One-way ANOVA of IgM_M9-Bg (A) or IgG_M9-Bg (B) by BPH, Gr3, and the Quartile Subgroups of Gr4/5 for the Subjects (n = 259) in the PSA "grey zone", that is, PSA Cutoff of 10 ng/mL

Level	- Level	Score mean difference	Std Err Dif	*Z*	*P*-value	Hodges–Lehmann	Lower CL	Upper CL
A. IgM_M9-Bg								
6_7.03-40.67	1_BPH	25.8918	9.700949	2.66900	0.0076*	0.089000	0.029000	0.1580000
5_3.99-7.021	1_BPH	21.9825	9.549432	2.30196	0.0213*	0.087000	0.015500	0.1685000
6_7.03-40.67	2_Gr3	12.0072	6.221564	1.92993	0.0536	0.061750	−0.001000	0.1276667
6_7.03-40.67	3_<0.91	11.9301	4.114149	2.89977	0.0037*	0.111000	0.043000	0.1840000
2_Gr3	1_BPH	11.2677	8.039948	1.40146	0.1611	0.026500	−0.010000	0.0650000
5_3.99-7.021	3_<0.91	10.1488	4.131895	2.45621	0.0140*	0.110000	0.023000	0.1995000
5_3.99-7.021	2_Gr3	9.3514	6.169023	1.51587	0.1296	0.062000	−0.017000	0.1430000
6_7.03-40.67	4_0.91-3.95	8.2353	3.465031	2.37669	0.0175*	0.121000	0.031000	0.1990000
5_3.99-7.021	4_0.91-3.95	7.2446	3.517090	2.05982	0.0394*	0.108000	0.004000	0.2300000
6_7.03-40.67	5_3.99-7.021	0.0000	3.560116	0.00000	1.0000	−0.000500	−0.109000	0.1020000
4_0.91-3.95	3_<0.91	−1.0730	4.099704	−0.26173	0.7935	−0.011500	−0.076000	0.0640000
3_<0.91	1_BPH	−6.8126	8.615290	−0.79076	0.4291	−0.020500	−0.070000	0.0260000
4_0.91-3.95	1_BPH	−8.3818	9.869202	−0.84929	0.3957	−0.028000	−0.093500	0.0390000
4_0.91-3.95	2_Gr3	−10.6058	6.282647	−1.68811	0.0914	−0.061250	−0.126000	0.0100000
3_<0.91	2_Gr3	−11.4636	5.941975	−1.92925	0.0537	−0.048500	−0.101000	0.0010000
B. IgG_M9-Bg								
6_7.03-40.67	1_BPH	34.5439	9.700962	3.56087	0.0004*	0.254000	0.112000	0.4450000
6_7.03-40.67	2_Gr3	19.9283	6.221528	3.20312	0.0014*	0.245500	0.080333	0.4670000
6_7.03-40.67	3_<0.91	13.4157	4.114030	3.26096	0.0011*	0.292500	0.117000	0.5270000
6_7.03-40.67	4_0.91-3.95	9.5507	3.465516	2.75591	0.0059*	0.271000	0.076000	0.5530000
6_7.03-40.67	5_3.99-7.021	9.1418	3.560327	2.56769	0.0102*	0.247000	0.049000	0.5135000
2_Gr3	1_BPH	8.6157	8.039948	1.07162	0.2839	0.024000	−0.022000	0.0690000
5_3.99-7.021	1_BPH	4.5132	9.549408	0.47261	0.6365	0.018000	−0.062000	0.1070000
5_3.99-7.021	3_<0.91	2.7877	4.132007	0.67465	0.4999	0.032000	−0.060000	0.1360000
5_3.99-7.021	4_0.91-3.95	1.8390	3.517090	0.52288	0.6011	0.037000	−0.080000	0.1630000
5_3.99-7.021	2_Gr3	−0.1375	6.169023	−0.02229	0.9822	−0.001500	−0.081000	0.0840000

Level	- Level	Score mean difference	Std Err Dif	*Z*	*P*-value	Hodges–Lehmann	Lower CL	Upper CL
4_0.91-3.95	3_<0.91	−0.4199	4.099830	−0.10241	0.9184	−0.004000	−0.099500	0.0925000
4_0.91-3.95	1_BPH	−3.1094	9.869229	−0.31506	0.7527	−0.012000	−0.091000	0.0660000
3_<0.91	1_BPH	−3.5685	8.615246	−0.41421	0.6787	−0.011000	−0.072000	0.0490000
4_0.91-3.95	2_Gr3	−5.4341	6.282647	−0.86493	0.3871	−0.032250	−0.117000	0.0500000
3_<0.91	2_Gr3	−6.1746	5.941928	−1.03916	0.2987	−0.034750	−0.098000	0.0330000

A nonparametric statistical test (Wilcoxon rank-sum method) was applied to calculate the significance of differences among subgroups. q* 1.95996, Alpha 0.05.